PHYSICAL REVIEW B VOLUME 14, NUMBER 11 1 DECEMBER 1976

Anomalous scattering and asymmetrical line shapes in Raman spectra of orthorhombic $KNbO_3$

A. M. Quittet
Laboratoire de Physique des Solides, Université Paris-Sud, Orsay, France

M. I. Bell
Physics Department, Yeshiva University, New York, New York

M. Krauzman
Département de Recherches Physiques, Laboratoire Associé au Centre National de la Recherche Scientifique No. 71, Université Paris VI, France

P. M. Raccah
Physics Department, Yeshiva University, New York, New York

(Received 27 May 1976)

The Raman spectrum of orthorhombic $KNbO_3$ is found to contain anomalous scattering, consisting of a large background and broad bands, which can be related directly to the dynamic disorder which has been invoked to explain the results of earlier studies of diffuse x-ray scattering and inelastic neutron scattering. Some ordinary first-order lines exhibit coupling to the anomalous part of the spectrum, which is revealed by the existence of resonant interference of the type described by Fano. All these features disappear abruptly at the transition to the low-temperature rhombohedral phase, indicating that they are characteristic of the peculiar dynamics of linear chains observed in the orthorhombic, tetragonal, and cubic phases.

INTRODUCTION

In the ferroelectric perovskites such as $BaTiO_3$ and $KNbO_3$, x-ray diffuse-scattering[1] and inelastic-neutron-scattering[2,3] experiments yield evidence of a very large anisotropy in the dispersion of some of the vibrational modes. Light scattering[4,5] has been used to investigate the zone-center phonons in order to check the soft-mode theories.[6] We report here some new results of Raman scattering experiments performed on a single-domain $KNbO_3$ sample, both in its room-temperature orthorhombic phase and as the temperature is lowered through the orthorhombic-to-rhombohedral phase transition.

The assignment of the ordinary first-order lines is quite easily obtained, leaving outside this classification a large continuous scattering which we refer to as "anomalous." The latter, previously described in Ref. 5 for restricted scattering geometries, has now been found to occur more generally whenever the incident and scattered beams propagate perpendicular to the Z axis and are simultaneously polarized parallel to Z. As expected, this anomalous spectrum disappears abruptly at the orthorhombic-to-rhombohedral transition temperature, as does the normal low-frequency B_2(TO) line. In the spectra where the anomalous scattering occurs, some first-order lines display an asymmetrical shape characteristic of a "Fano interference."[7]

EXPERIMENTAL

The Raman scattering was excited by an argon-ion laser operating at either 4880 or 5145 Å. Measurements were made using a $\frac{1}{4}$-m Spex double-grating spectrometer located at the Maybaum Institute of Yeshiva University and a Coderg T800 triple-grating spectrometer located at Département de Recherches Physiques, Université Paris VI. Both systems employed photon-counting detection.

We used a single-domain sample cut with the faces perpendicular to the orthorhombic axes. Standard right-angle and backscattering geometries were used to obtain various linear momentum transfers from the photons to the crystals. Table I summarizes the modes which can be observed in each scattering geometry. The orthorhombic axes are related to the pseudocubic ones as described in Fig. 1. At zero wave vector, the irreducible representations of the 12 optic modes in the C_{2v} point group of the orthorhombic phase are as follows: $4A_1(X)$, $4B_1(Y)$, $3B_2(Z)$, $1A_2$. All A_1, B_1, and B_2 modes are infrared active (the letters in parentheses indicate the direction of the dipole moment of each mode), and for these the longitudinal or transverse character must be considered. Two features of this table should be noted. First, B_1 and B_2 modes are not detected in a longitudinal configuration. Second, when a polar mode is neither transverse nor longitudinal

TABLE I. Summary of the scattering geometries employed and the mode symmetries observed. Scattering geometries are indicated by the conventional notation $\vec{k}_i(\vec{\epsilon}_i\vec{\epsilon}_s)\vec{k}_s$, where $\vec{k}_i, \vec{\epsilon}_i$ ($\vec{k}_s, \vec{\epsilon}_s$) are the wave vector and polarization vector of the incident (scattered) photon.

				Polarization of incident and scattered beams ($\vec{\epsilon}_i\vec{\epsilon}_s$) and mode symmetry					
	Incident wave vector	Scattered wave vector	Momentum transfer	XX	YY	ZZ	YX,XY	ZX,XZ	YZ,ZY
	$\vec{k}_i$	$\vec{k}_s$	$\vec{k}_s-\vec{k}_i$	A_1	A_1	A_1	B_1	B_2	A_2
Right-angle scattering	X	Y	$\perp Z$	···	···	Mixed	Mixed	TO	Indiff.
	Y	Z	$\perp X$	TO	···	···	Mixed	Mixed	Indiff.
	X	Z	$\perp Y$	···	Mixed	···	TO	Mixed	Indiff.
Backscattering	X	$\bar{X}$	$\parallel X$	···	LO	LO	···	···	Indiff.
	Y	$\bar{Y}$	$\parallel Y$	TO	···	TO	···	···	···
	Z	$\bar{Z}$	$\parallel Z$	TO	TO	···	TO	···	···

in a given scattering geometry (labeled "mixed"), it loses its zero-wave-vector irreducible-representation species through mixing with modes of different symmetry.

ROOM-TEMPERATURE SPECTRA

All the spectra listed in Table I have been recorded. Only those of special interest are reproduced in Figs. 2 and 3. In Fig. 2, the peaks which arise from contamination by other species are drawn with broken lines.

From Table I, and taking into account the possible mixing of species, we can assign the observed frequencies to the different modes. These assignments are summarized in Table II. Within the limit of experimental accuracy, we agree with the results published independently by Winter *et al.*,[5] at least for those lines identified unambiguously in Ref. 5. The following details should be noted. The low-frequency B_2(TO) line (maximum at 40 cm^{-1}) is broad and asymmetrical [Fig. 2(a)], and a thin line at 195 cm^{-1} which sits on its tail is slightly distorted and seems to show a dip on the low-frequency side. In the B_2 mixed spectrum, the lines at 170 and 205 cm^{-1} display an interference dip between them [Fig. 2(b)].

The anomalous spectrum is seen in the following geometries: $Y(ZZ)\bar{Y}$, $X(ZZ)\bar{X}$, and $X(ZZ)Y$. These are A_1(TO), A_1(LO), and A_1(mixed) spectra, respectively, and are shown in Figs. 3(e), 3(a), and 3(c). In each case, the linear momentum transfer is perpendicular to the Z axis, and the light beams are polarized parallel to Z. The anomalous scattering, identical in the three spectra, consists of a continuous background, decreasing in intensity from low to high frequency, and two broad bumps centered near 130 and 430 cm^{-1}.

The ordinary first-order lines are superimposed on the anomalous spectrum, but some of them show a coupling leading to an asymmetrical lineshape and interference dip. This is clearly demonstrated by comparison of the pairs of spectra in Fig. 3:

(i) Figures 3(a) and 3(b): The normal $X(YY)\bar{X}$

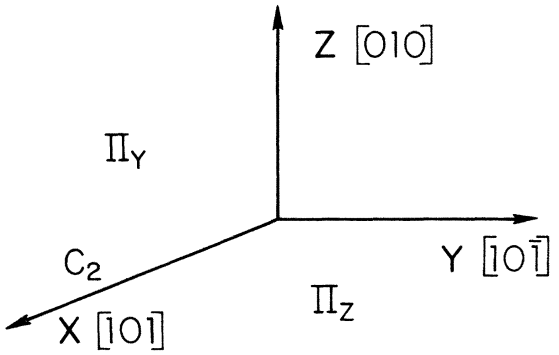

FIG. 1. Orthorhombic axes for $KNbO_3$ and corresponding pseudocubic axes (in brackets). Also shown are the symmetry elements of the C_{2v} point group. The spontaneous polarization is in the X direction.

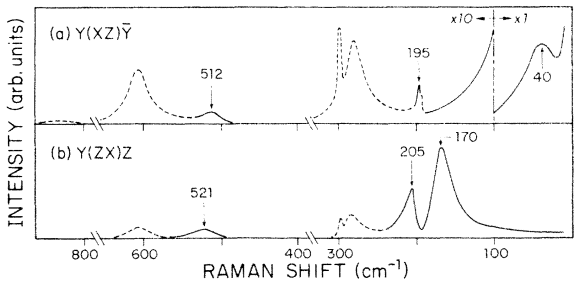

FIG. 2. B_2 symmetry spectra: (a) B_2(TO) in backscattering geometry, (b) B_2 (mixed) in right-angle geometry. The dashed lines indicate contamination from other symmetry species due either to a small misorientation of the polarizers or to mixing of polar modes as described in the text.

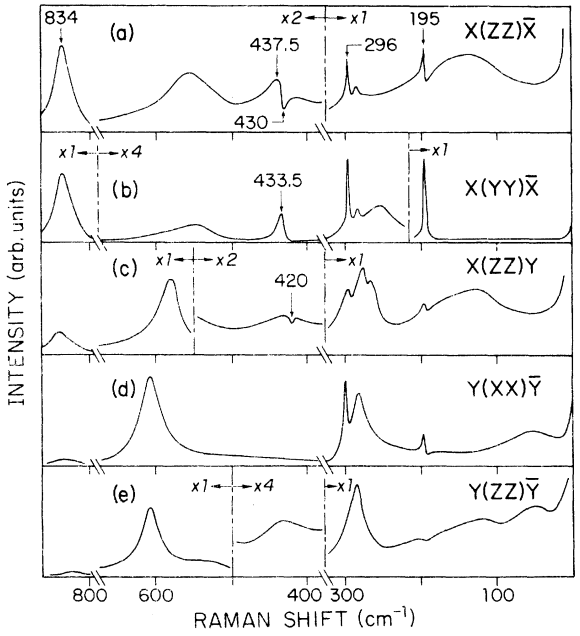

FIG. 3. Anomalous spectra and the associated normal spectra. In the $Y(XX)\bar{Y}$ and $Y(ZZ)\bar{Y}$ spectra, the broad line in the vicinity of 50 cm^{-1} is most probably a contamination from the $Y(XZ)\bar{Y}$ B_2(TO) spectrum due to the divergence of the scattered beam.

spectrum together with the anomalous $X(ZZ)\bar{X}$ one are both A_1(LO) spectra. Note the lines at 195 and 435 cm^{-1}.

(ii) Figures 3(d) and 3(e): The normal $Y(XX)\bar{Y}$ spectrum together with the anomalous $X(ZZ)\bar{Y}$ one are both A_1(TO) spectra. Note the line at 193 cm^{-1}.

(iii) Figure 3(c): The anomalous $X(ZZ)Y$ spectrum has A_1 (mixed) symmetry. Note the mode at

TABLE II. Frequencies and symmetry assignments of first-order Raman lines of $KNbO_3$. The figure in parentheses is the full width of the line at half-maximum.

A_1(TO)	A_1(LO)	B_1(TO)	B_2(TO)	A_2
			40(27×2)	
193(2)	194.5(3)	192(2)	1.96.5[a]	
		249(25)		
		270		
281.5(33)				282(6)
	295(5)			
297(5)				
	434.5[a](10)			
			513(20)	
		534(20)		
606.5(33)				
	834(27)			

[a] Lines showing an asymmetrical shape in at least one scattering geometry.

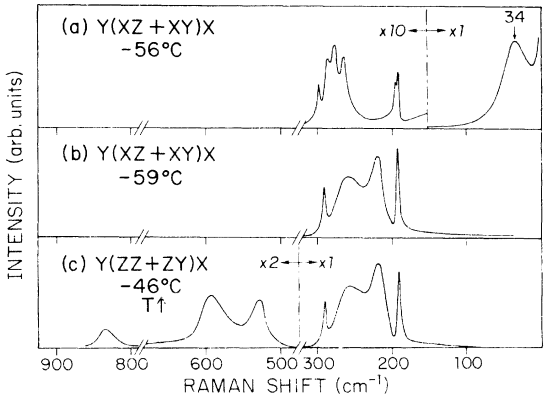

FIG. 4. Temperature dependence of part of the $B_1 + B_2$ spectrum: (a) in the orthorhombic phase just above the phase transition (temperature decreasing), (b) in the rhombohedral phase just below the transition (temperature decreasing), (c) in the rhombohedral phase in the hysteresis interval (temperature increasing).

420 cm^{-1} which appears almost wholly negative in the anomalous part of the spectrum.

TEMPERATURE DEPENDENCE (REF. 8) (23 to −70 °C)

As the temperature is lowered, there is essentially no change in the low-frequency B_2(TO) line and the anomalous spectrum until the transition temperature is reached. The frequency and width of the B_2 line both decrease slightly, but its intensity [Fig. 4(a)], as well as the shape and intensity of the anomalous spectrum, remains unchanged. Below the phase transition, which takes place near −59°C, the spectrum becomes very different [Figs. 4(b) and 4(c)] as the broad B_2 line and the anomalous scattering disappear completely. Since the sample becomes broken and twinned, all the spectra are superimposed, so that it is not possible to miss any lines. Upon reheating the sample, the anomalous spectra of the orthorhombic phase appear again at −30 °C, exhibiting the large thermal hysteresis characteristic of a first-order transition. These experiments thus demonstrate that the anomalous spectrum is related to an intrinsic property of the orthorhombic phase, as is the low-frequency B_2(TO) line.

DISCUSSION

We note first that all the anomalous features which appear in Raman, neutron, and x-ray scattering experiments occur only when the linear momentum transfer lies perpendicular to the Z axis, and that these features disappear in the rhombohedral phase. Hence the dynamical properties of the orthorhombic phase have a pronounced one-dimensional character. These results can be

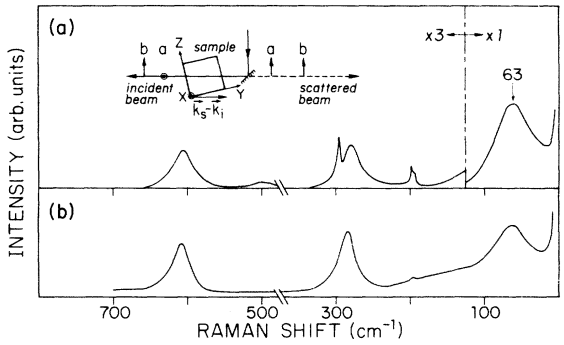

FIG. 5. (a) B_2 spectrum for a momentum transfer rotated by 15° from a TO configuration toward the LO configuration. (b) Anomalous spectrum for the same momentum transfer.

understood[1] as arising from displacements of the niobium atoms in the Z direction (away from the C_2 symmetry axis) which are correlated for some finite distance along Z. Averaged over distances large compared to this correlation length, however, the structure retains orthorhombic symmetry. Such disorder need not be static, since its effects will be seen in scattering experiments provided the lifetime of the local departure from the average symmetry is greater than the scattering time. From this point of view, the anomalous features in the Raman spectra can be interpreted as disorder-induced first-order scattering, i.e., one-phonon scattering by modes which would not be Raman active in a perfect crystal, but which become so when both the translational and point-group symmetries are broken by the disorder. Since all phonons (not only those at the zone center) can become Raman active in this way, one anticipates a scattering spectrum proportional, in first approximation, to the one-phonon density of states. This interpretation is further strengthened by the fact that neutron scattering results[3] suggest the existence of a peak in the one-phonon density of states near 150 cm^{-1}, close to one of the peaks (130 cm^{-1}) in the anomalous Raman spectra.

We have studied the modification of the spectra which occurs as the linear momentum transfer is rotated from the Y direction to the Z direction. As the momentum transfer is changed, the intensity of the anomalous scattering decreases rapidly, while the frequency of the B_2 line shifts very rapidly toward higher values [Figs. 5(a) and 5(b)]. We conclude from this that the B_2 line is produced by an underdamped zone-center phonon with a large LO-TO frequency difference and that the anomalous spectrum in ZZ polarization arises from a continuum of states. Our identification of the line at 40 cm^{-1} as the zone-center B_2(TO) phonon is consistent with the results of neutron scattering experiments.[3] Although Currat *et al.*[3] extrapolate the frequency of the optical branch to about 25 cm^{-1} at the zone center, the experimental resolution is such that spectra near the zone center and at low frequencies are always heavily contaminated by the Bragg peak and the acoustic dispersion. Moreover, the experimental points closest to the zone center could only be obtained from constant-energy scans which do not provide an accurate measure of mode frequency.

The asymmetrical line shapes observed in this work are of two types. One is produced by the small interference between the two lowest-lying lines in the B_2(TO) spectrum [Fig. 2(a)]. This is merely a coupling between modes of identical symmetry, which appears because of the large width of the low-frequency line. The coupling becomes much stronger when the wave vector is rotated 45° from the Y axis toward the Z axis, since the rapid increase in the frequency of the lower mode brings the two modes quite close [Fig. 2(b)].

The second type of asymmetry can be seen in the shape of several narrow lines observed in the anomalous ZZ spectra. This can be analyzed, using a formalism developed by Fano,[7] as an interference between the scattering by a discrete, one-phonon state and a continuum of states. Such line shapes have been reported previously in $BaTiO_3$ by Rousseau and Porto[9] and in heavily doped silicon by Cerdeira *et al.*[10] The application of Fano's formalism to Raman scattering has been treated in detail by Scott.[11] If the Hamiltonian H couples a discrete state φ with a continuum ψ_E according to

$$\begin{aligned} &\langle \varphi | H | \varphi \rangle = E_\varphi , \\ &\langle \psi_E | H | \varphi \rangle = V_E , \\ &\langle \psi_{E'} | H | \psi_E \rangle = E\delta(E - E') , \end{aligned} \tag{1}$$

then the observed scattering cross section σ is related to the cross section σ_E which would be produced by the continuum in the absence of any coupling by

$$\sigma = [(q + \epsilon)^2/(1 + \epsilon^2)]\,\sigma_E . \tag{2}$$

Here $\epsilon = (E - E_\varphi - \delta E)/\Gamma$ is a reduced energy variable involving the half-width $\Gamma = \pi |V_E|^2$ and energy shift $\delta E = \pi^{-1} \mathrm{P} \int dE'\, \Gamma/(E - E')$ (P indicates "principal part of") of the "resonant" state resulting from the discrete-continuum interaction. The parameter $q = (\pi V_E)^{-1} \langle \Phi | \alpha_{ij} | i \rangle / \langle \psi_E | \alpha_{ij} | i \rangle$ depends on the matrix elements of the Raman tensor α_{ij} for transitions from an initial state $|i\rangle$ to the continuum ψ_E and to the state $\Phi = \varphi + \mathrm{P} \int dE'\, V_{E'} \psi_{E'} / (E - E')$, which is the discrete state φ modified by

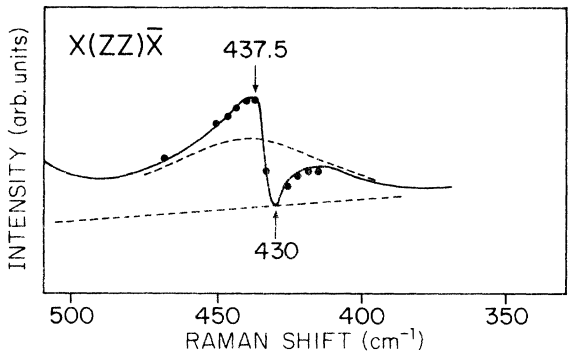

FIG. 6. Comparison of the experimental $X(ZZ)\bar{X}$ spectrum (solid curve) with the prediction of Eq. (2) (dots).

an admixture of continuum states. If q and Γ are independent of E in a sufficiently large interval around E_φ, the spectrum can be fitted to Eq. (2) with q and Γ treated as (energy-independent) fitting parameters. (Note that Γ and q cannot be completely independent of energy unless $\delta E = 0$.) Figure 6 compares the experimental $X(ZZ)\bar{X}$ spectrum near 430 cm^{-1} with the prediction of Eq. (2) to which a slowly varying background has been added. A good fit is obtained for $q = 0.75$, $\Gamma = 3.6$ cm^{-1}, $E_\varphi + \delta E = 432.7$ cm^{-1}. The value of E_φ obtained from the $X(YY)\bar{X}$ spectrum [Fig. 3(b)] is 430 cm^{-1}, yielding a shift $\delta E = 2.7$ cm^{-1} due to the coupling. The exact nature of this coupling remains to be determined. If, as we have proposed, the continuum is produced by disorder-induced first-order scattering, it may be coupled to zone-center modes via anharmonic terms in H as discussed by Scott[11] or via additional terms which depend directly on the disorder.

CONCLUSION

The experiments described here demonstrate that a major part of the dynamical behavior of orthorhombic $KNbO_3$ is one dimensional in character and consistent with the formation of linear chains of correlated displacements of niobium ions as proposed in connection with diffuse x-ray scattering results[1] and Raman scattering studies of the cubic and tetragonal phases.[5] This further evidence of disorder in the orthorhombic phase, together with the observation that the lowest B_2(TO) mode does not display any significant softening with decreasing temperature, strongly suggests that the phase transitions of $KNbO_3$ (including the ferroelectric-paraelectric one) have some order-disorder character. Such a suggestion is not inconsistent with the fact that the transitions are thermodynamically of first order, since recent studies[12] of systems of dipoles interacting via a generalized molecular field have shown that first-order transitions are possible in such a model and that an accurate quantitative description of the cubic-tetragonal transition in $BaTiO_3$ can be obtained.

ACKNOWLEDGMENTS

We are indebted to U. Fluckinger of the Laboratorium für Festkörperphysik, ETH Zurich who provided us with the excellent single-domain $KNbO_3$ sample, to Professor M. Lambert for helpful discussions, and to G. Hamel for technical assistance. The work at Yeshiva University was supported by the Advanced Research Projects Agency.

[1] M. Lambert and R. Comès, Solid State Commun. 7, 305 (1969).
[2] A. C. Nunes, J. D. Axe, and G. Shirane, Ferroelectrics 2, 291 (1971).
[3] R. Currat, R. Comès, B. Dorner, and E. Wiesendanger, J. Phys. C 7, 2521 (1974).
[4] M. P. Fontana and M. Lambert, Solid State Commun. 10, 1 (1972); M. DiDomenico, Jr., S. H. Wemple, S. P. S. Porto, and R. P. Bauman, Phys. Rev. 174, 522 (1968); D. Heiman and S. Ushioda, Phys. Rev. B 9, 2122 (1974).
[5] A. M. Quittet, M. Fontana, M. Lambert, and E. Wiesendanger, Ferroelectrics 8, 585 (1974); F. X. Winter, E. Wiesendanger, and R. Claus, Phys. Status Solidi B 64, 95 (1974).
[6] P. Anderson, in *Proceedings All-Union Conference on the Physics of Dielectrics* (Acad. Sci. USSR, Moscow, 1958), p. 209; W. Cochran, Adv. Phys. 9, 387 (1960) and 10, 401 (1961).
[7] U. Fano, Phys. Rev. 124, 1866 (1961).
[8] Similar results have been reported recently by M. P. Fontana and C. Razzetti [Solid State Commun. 17, 377 (1975)].
[9] D. L. Rousseau and S. P. S. Porto, Phys. Rev. Lett. 20, 1354 (1968).
[10] F. Cerdiera, T. A. Fjeldly, and M. Cardona, Phys. Rev. B 8, 4734 (1973).
[11] J. F. Scott, Phys. Rev. Lett. 24, 1107 (1970); Rev. Mod. Phys. 46, 83 (1974).
[12] M. I. Bell and P. M. Raccah, Bull. Am. Phys. Soc. 20, 349 (1975); Yeshiva University Technical Report No. ECOM-74-0470-1 (1975) (unpublished).